焊接顺序对整体叶盘圆度影响的有限元分析

张学秋[1,3]， 杨建国[1,2]， 刘雪松[1]， 陈绪辉[1]， 方洪渊[1]， 曲 伸[2]

（1. 哈尔滨工业大学 现代焊接生产技术国家重点实验室，哈尔滨 150001；
2. 沈阳黎明航空发动机集团有限责任公司，沈阳 110043；3. 上海宝钢集团，上海 201900）

摘 要：采用多种软件的综合运用建立了整体叶盘的有限元模型，并基于焊接过程中温度之间相互影响程度选取了顺序依次焊接、90°和 180°三种典型的焊接顺序，通过有限元分析的方法对不同焊接顺序产生的变形进行计算和分析. 结果表明，以往使用的 180°最远距离焊接顺序并不是最合理的焊接顺序，在相同的焊接工艺条件下，顺序依次焊接对整体叶盘圆度的影响相对较小. 该分析结果说明在材料不同、焊接方法及结构不同的情况下，焊接顺序没有固定的模式，为整体叶盘及大型复杂结构件焊接顺序的合理选择提供了理论依据.

关键词：焊接顺序；变形；温度场；残余应力

中图分类号：TG444 文献标识码：A 文章编号：0253－360X(2010)03－0057－04

张学秋

0 序 言

20世纪 80年代中期美国制定“ IHPTET计划”，该计划预计耗资 50亿美元，经过 15年左右的时间使航空燃气涡轮发动机的性能成倍提高，推重比达到 15～20，耗油下降 30%～50%[1]，从这个时期开始，全球化的竞争要求航空发动机生产厂家尽可能地缩短研发周期，降低成本及市场风险，由于计算机仿真可以替代大量试验，特别是在发动机早期设计阶段可以用较少的投资获得几种不同的设计方案，因而得到日益广泛的应用[2－4]. 对于航空发动机整体叶盘而言，由于其模型构造复杂，整体叶盘焊接多达 40道焊缝，若要每道焊缝自由排列将是一个天文数字，要是全部计算几乎是不可能的，因此，如何合理的设计焊接顺序方案以达到控制变形的最佳效果显得非常重要. 采用试验的方法去验证焊接顺序将花费高额成本，也不现实. 因此根据整体叶盘的实际工艺参数对三种典型的焊接顺序的径向变形进行了有限元分析，以期优选合理的焊接顺序.

1 有限元模型的建立

1.1 有限元模型

大型复杂结构的有限元建模是数值模拟分析中的一个非常重要的环节，也是一个较难处理的环节，因为不但要考虑计算准确性，还要考虑计算机的承受能力，整体叶盘电子束的焊缝宽度仅为 2 mm，而叶盘的外径已达到 700 mm，这对建模的影响非常大，在这个跨度下，要完成一个符合标准的有限元模型是非常困难的. 此外，叶片是带有一定角度的曲面，在 Marc前处理中也很难实现，因此在叶盘的建模过程中借助了机械辅助设计软件 UG建立了三维模型，导入到 Hypermesh中通过平面的修补和网格的重划分技术[5,6]，对焊缝及其附近处的单元进行了细分，对离焊缝较远的单元进行了粗化，其有限元模型分别如图 1和图 2所示. 这样单元的数目得到了大量降低，且保证了计算的精度，按此方法处理后整体叶盘的有限元模型如图 3所示，共计 189 092个单元，121 770个节点.

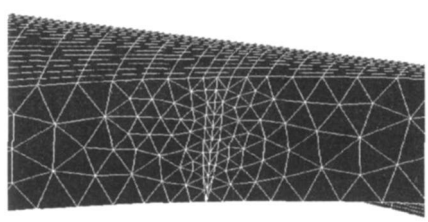

图 1 焊缝细分处的有限元模型

Fig. 1 Finite element model of weld position

1.2 整体叶盘材料

TC4是 20世纪 50年代发展起来的一种中等强

收稿日期：2008－12－23

基金项目：中国博士后科学基金资助项目（20070410900）；黑龙江省博士后基金项目（LBH－Z07129）

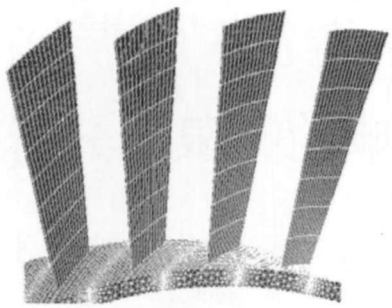

图 2 整体叶盘叶片粗化的有限元模型

Fig. 2 Finite element model of blades

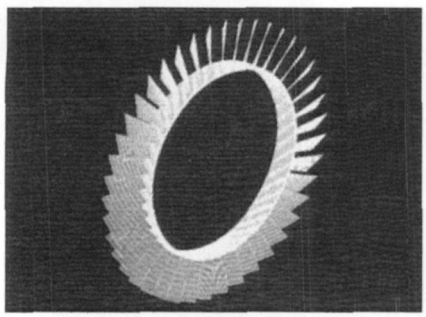

图 3 整体叶盘有限元模型

Fig. 3 Finite element model of blisk

度的 α-β 两相型钛合金，它含有 6%的 α 稳定元素 Al 和 4%的 β 稳定元素 V[7]. 由于其优良的力学性能和良好的焊接性，在航空航天领域得到了广泛的应用. 其化学成分如表 1所示.

表 1 TC4钛合金的化学成分(质量分数，%)

Table 1 Chemical element of TC4 titanium alloy

O	Al	V	Fe	C	N	H	Ti
0.063	5.82	3.99	<0.05	0.019	0.003 2	0.000 7	余量

1.3 焊接热源模型的确定

由于焊接方法为真空电子束焊接，其具有加热功率密度大、焊接速度快、焊接冶金质量好、焊缝窄、焊缝深宽比大、焊缝及热影响区晶粒细、焊接厚板时效率高和保护可靠等优点，在钛合金的焊接中得到了广泛应用. 其焊缝的截面形貌类似于“钉”形，过去在热源模型的选择上进行了多方面的研究和讨论，采用圆锥形、移动双椭球及圆柱形热源模型等方法来模仿电子束焊接的截面形状，文中采用了高斯面热源模型和椭球形移动热源叠加应用的方法，高斯面热源模型的表达式为

$$q(r)=q(0)\,e^{-cr^2} \tag{1}$$

式中：$q(r)$为半径 r处的表面热流；$q(0)$为热源中心处热流量最大值；c为热源集中系数；r为距热源中心的距离[8].

椭球形移动热源模型的表达式为

$$q(x,y,z,t)=\frac{6\sqrt{3}\eta UI}{\pi abc\sqrt{\pi}}e^{-3x^2/a^2}e^{-3y^2/b^2}e^{-3[z+v(\tau-t)]^2/c^2} \tag{2}$$

式中：η为热源有效系数；U为电弧电压；I为焊接电流；a、b、c为椭球尺寸参数；v为焊接速度；τ为焊接热源的滞后时间[9]；t为焊接时间.

2 焊接顺序方案确定

不同的焊接顺序将产生不同的温度热循环，而由此产生的温度应力和变形也会有所不同，例如按顺时针顺序依次焊接，由于温度热循环的作用，在下一道焊缝施焊时的初始温度已经由于上一道焊缝的影响达到一定的温度，而且随着焊接过程的进行，后焊焊缝的初始温度会越来越高，各条焊缝之间温度的相互影响就越来越大，怎样才能使温度之间的影响更加趋于合理是一个很复杂的问题，在众多的焊接顺序上寻找合理的焊接顺序就要根据实际工作经验入手，找出几种相对合理的焊接顺序，通过有限元计算的方法，对最后的变形计算结果进行对比分析，找到较合理的一种焊接顺序.

在整体叶盘典型焊接顺序的选择上，选择的原则是建立在温度影响最小的基础上，就是下一条焊缝焊接时尽量使其焊接时受已焊焊缝温度场的综合影响最小，比如在整体叶盘的圆周上，如果定义第一条焊缝所在的位置为 0，那么按最远的距离计算，在圆周上顺时针旋转 180°的所在位置，应该是与第一条焊道为最远距离，因此按此想法第三条焊缝应该在 90°或 270°，为了便于清晰区分这种排列与其它排列的不同，将这种第一道焊缝与第二道焊缝相隔的角度 180°命名为 180°排列法.

按照这种排列的思想，焊接顺序是有规律可寻的，因为如果焊道完成一周作为一个循环，180°排列法每一循环仅包含二条焊缝，90°排列法则每一循环包含四条焊缝，所以推导到若以 N°为间隔，即 N°排列法，则每一循环包含的焊缝为 360/N，如果不是整数，则按四舍五入法确定，下一循环遵循的准则为上一循环二条焊道的中间焊道，即以一周作为一个循环，第一循环按间隔角度不同计算后得到的焊接顺序如果为 n_1，n_2，n_3，…n_k，则第二循环的焊道顺序为 m_1，m_2，m_3，…m_{k-1}，$m_1=(n_1+n_2)/2$，$m_2=(n_2+n_3)/2$…，$m_{k-1}=(n_{k-1}+n_k)/2$，按此规律不但可以验证上述 180°排列法，同时可以求得 90°排列法的焊接顺序，在焊接顺序的选取上，由于要对比所选

顺序的焊接变形效果优劣，因此选取了顺时针依次焊接的方案作为对比．按照上述的焊接顺序对整体叶盘电子束焊接进行数值分析，对比各焊接顺序下叶片的变形情况，综合分析求出合理的焊接顺序．

3　焊后叶盘圆度的计算结果

在焊接顺序的分析中，由于模拟过程中缺省的坐标为笛卡尔直角坐标系，而整体叶盘为圆筒形结构，所以在后处理中利用了坐标转换法，将直角坐标系转换为柱坐标系．坐标转换后，顺序焊接径向位移的变化云图如图 4所示．由于是研究焊接顺序对叶盘圆度的影响，根据计算结果，取叶盘根部沿轴向中心截面上径向位移进行数据采集，如图 5所示．

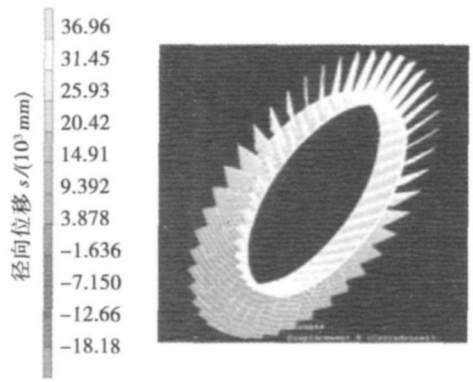

图 4　顺序焊接径向位移的变化云图

Fig. 4　Contour bands of radial displacement change (welding in turn)

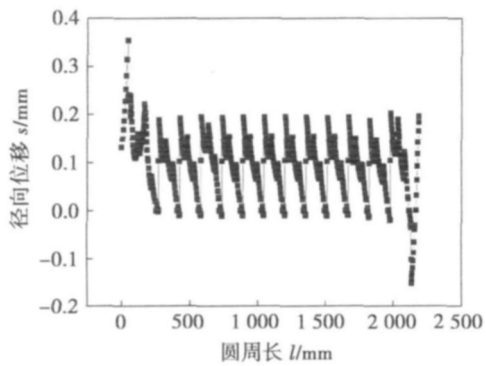

图 5　叶片根部径向位移的变化

Fig. 5　Radial displacement change of blade root

径向位移最大值为 0.370 mm，最小值为 −0.182 mm(图 5)，由于叶盘的内径为 620 mm，根据圆度的公式(3)可得按顺序焊接方法圆度为 0.09%．

$$e=\frac{D_{max}-D_{min}}{(D_{max}+D_{min})/2}\times 100\% \qquad (3)$$

式中：e为圆度；D_{max}为圆盘外径最大值；D_{min}为圆盘外径最小值．

90°排列和 180°排列焊接径向位移变化云图分别如图 6和图 7所示，根据顺序焊依次焊接计算圆度的方法，可以计算出 90°排列和 180°排列所得整体叶盘圆度的结果分别为 0.107%和 0.108%．

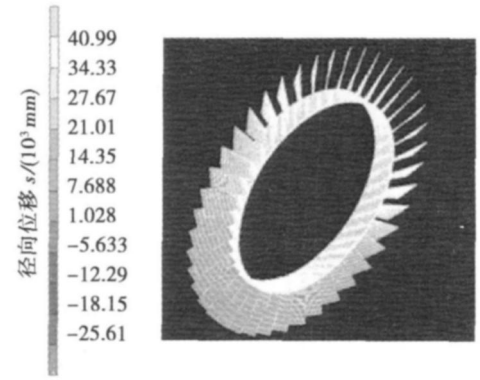

图 6　90°径向位移的变化云图

Fig. 6　Contour bands of radial displacement change (90° welding sequence)

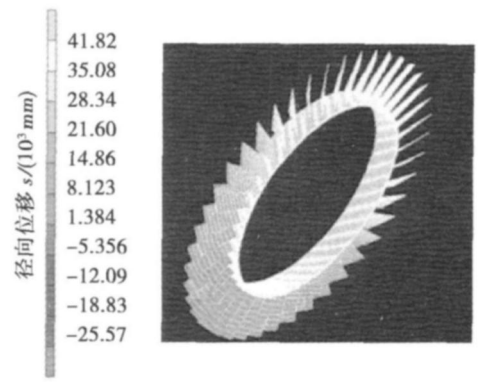

图 7　180°径向位移的变化云图

Fig. 7　Contour bands of radial displacement change (180° welding sequence)

在整体叶盘的实际焊接中，普遍采用的是 180°排列顺序，但是从计算的结果来看，实际上 180°焊接排列顺序对叶盘圆度的影响并不是最小的，因为虽然在焊接初始阶段，焊道间保持了最远的距离，温度的影响肯定最小，这点是勿庸质疑的，但是由于焊缝的数量较多，相互关系错综复杂，特别是对于这种多焊缝情况．此外，电子束焊接是在真空中进行，只能以辐射的形式散热，这样散热速度非常缓慢，也是导致该结果的一个因素．因此，从上述分析可知，在三种典型的焊接顺序中，依次焊接的方法对圆度的影响是最小的．所以对于圆度要求较高的整体叶盘或其它的侧壁有焊道的圆形精密仪器，在没有找到

更好的焊接顺序以前，应采用顺序依次焊接的方法来代替 180°焊接排列顺序.

4 结 论

(1)采用 Hypermesh平面修补技术和网格重划分技术完成了整体叶盘有限元建模，保证了计算精度，节约了计算时间.

(2)在三种典型焊接顺序对圆度影响的有限元分析中，顺时针依次顺序焊接时的圆度为 0.09%，90°排列和 180°排接所得整体叶盘圆度的结果分别为 0.107%和 0.108%. 顺时针依次焊接对圆度的影响相对较小.

参考文献：

[1] Bayt Robert L, Sahm Michael K, Lents Charles E. Collaborative engineering in integrated aircraft power system design[C] // In ASME 2002 Design Engineering Technical Conferences and Computers and Information in Engineering Conference. Montreal, Canada, 2002: 1—5.

[2] Dutta A, Venugopal R A. Simulation of isothermal forging of compressor disc by combined numerical and physical modeling techniques[J]. Journal of Materials Processing Technology, 1997, 72(3): 392—395.

[3] Kohl M, Dhondt G, Broede J. Axisymmetric substitute structures for circular disks with noncentral holes[J]. Computer & Structures, 1996, 60(6): 1047—1065.

[4] Berglund D, Alberg H, Runnemalm H. Simulation of welding and stress relief heat treatment of an aero engine component[J]. Finite Elements in Analysis and Design, 2003, 39(9): 865—881.

[5] 于开平，周传月，谭惠丰. Hypermesh从入门到精通[M]. 北京：科学出版社，2005.

[6] 陈火红，尹伟奇，薛小香. MSC.Marc二次开发指南[M]. 北京：科学出版社，2004.

[7] 许鸿吉，尹丽香，李晋炜，等. TC4钛合金电子束焊接接头组织和性能[J]. 焊接学报，2005, 26(11): 43—46.
Xu Hongji, Yin lixiang, Li Jinwei, et al. Microstructures and properties of TC4 alloy joints welded by the electron beam welding[J]. Transactions of the China Welding Institution, 2005, 26(11): 43—46.

[8] Pavelic V, Tanbakuchi R, Auyehara O. Experimental and computed temperature histories in gas tungsten arc welding of thin plates[J]. Welding Journal Research Supplement, 1969, 48(7): 295—305.

[9] Goldak J, Chakravarti A, Bibby M. A new finite model for welding heat sources[J]. Metallurgical Transactions, 1984, B15: 299—305.

作者简介：张学秋，男，1973年出生，博士研究生. 主要从事数值模拟方面的研究. 发表论文 10篇.

Email: jackeee90@163.com

[上接第 56页]

Wang Zhechang. Discussion on principle of welding stress and distortion (I)[J]. Transactions of the China Welding Institution, 2008, 29(6): 73—76

[12] 王者昌. 焊接应力变形原理若干问题的探讨(二)[J]. 焊接学报，2008, 29(7): 69—72
Wang Zhechang. Discussion on principle of welding stress and distortion (II)[J]. Transactions of the China Welding Institution, 2008, 29(7): 69—72

[13] 汪建华，陆 皓，魏良武. 固有应变有限元法预测焊接变形理论及其应用[J]. 焊接学报，2002, 23(6): 36—40
Wang Jianhua, Lu Hao, Wei Liangwu. Prediction of welding distortions based on theory of inherent strain by FEM and its application[J]. Transactions of the China Welding Institution, 2002, 23(6): 36—40

[14] 方鸿渊，张学秋，杨建国，等. 关于焊接塑性应变的计算与讨论[J]. 焊接学报，2008, 29(7): 60—63.
Fang Hongyuan, Zhang Xueqiu, Yang Jianguo, et al. Calculation and discussion of welding plastic strain[J]. Transactions of the China Welding Institution, 2008, 29(7): 60—63.

[15] 方鸿渊，张学秋，杨建国，等. 焊接应力场与应变场的计算与讨论[J]. 焊接学报，2008, 29(3): 129—132.
Fang Hongyuan, Zhang Xueqiu, Yang Jianguo, et al. Calculation and discussion of welding stress and strain field[J]. Transactions of the China Welding Institution, 2008, 29(3): 129—132.

作者简介：李 菊，女，1970年出生，博士，高级工程师. 主要从事焊接应力与变形的控制研究工作. 发表论文 10余篇.

Email: lijuxin@yahoo.com

University, Xi'an 710049, China). p. 37 - 40

Abstract: A numerical calculation model with local refined mesh for laser deep penetration welding of titanium alloy is presented. A Rotatry-Gauss body heat source model was established to accurately describe the shape of keyhole and molten pool of the laser welded joint. The profile of keyhole and molten pool as well as the distribution of high gradient residual stresse are obtained. It is showed that the region of high stress locates in the keyhole region, and high gradient residual stress distributes in the other region of welded seam. The stresse gradient increases in the state of excessively high and low level of energy density as well as the state of lower linear energy. It is supposed that keeping the laser energy density in state of low and medium level or keeping the linear energy in state of low level could avoid the high gradient stresses.

Key words: high gradient residual stresses; energy density; linear energy; keyhole

Research on melting metal behavior of ultrasonic-tungsten inert gas welding. SUN Qingjie, YANG Chunli, LIN Sanbao, FAN Yangyang (State Key Laboratory of Advanced Welding Production Technology, Harbin Institute of Technology, Harbin 150001, China). p. 41 - 44

Abstract: The mechanism of melting behavior of metal under ultrasonic-tungsten inert gas (U-TIG) welding was studied. The results indicate that U-TIG welding can significantly enhance the arc force and electromagnetic convection, change the metal flow behavior, and increase the penetration and the ratio of depth to width. This method extends the application range and improves production efficiency of ordinary TIG welding. Besides, the mechanism of arc force enhancing and penetration increasing were also presented in combination with experiment and theoretical analysis.

Key words: ultrasonic-tungsten inert gas welding; arc force; arc shape; melting behavior

Effect of spray parameters on microstructure of plasma sprayed wollastonite coatings. HUANG Qing, WANG Weize, WAN Lei, XUAN Fuzhen (Key Lab of Safety Science of Pressurized System, Ministry of Education, School of Mechanical and Power Engineering, East China University of Science and Technology, Shanghai 200237, China). p. 45 - 48

Abstract: Wollastonite coating was prepared by plasma spraying at different spraying distances, primary gas flow rates and plasma power. The microstructure of the coating lager was examined by scanning electron microscope (SEM). The results show that the three spraying parameters affect the microstructure of wollastonite coatings greatly. Flatten degree of molten powder decreased and the number of pores increased with the increment of spraying distance at larger flow rate of primary gas. However, flatten degree of molten powder firstly increased and then decreased with the spraying distance at the lower flow rate of primary gas. The microstructure of coatings is denser with larger gas flow rate. Flatten degree increased with plasma power up to 36 kW. Further increase of plasma power results in more round pores appearing in coatings. Effect of spray parameters on the microstructure of wollastonite coatings mainly resulted from the influence on velocity and temperature of the molten droplets.

Key words: plasma spraying; wollastonite coating; spraying distance; plasma power; gas flow rate

Influence of transverse alternative magnetic field on microstructure and properties of plasma arc surfacing layer. LIU Zhengjun, ZHAO Qian, SONG Xingkui, YANG Yang (School of Material Science and Engineering, Shenyang University of Technology, Shenyang 110870, China). p. 49 - 52

Abstract: In the research of the influence of alternative pulsed magnetic field on microstructure and properties of nickel-base alloy, a transverse alternative pulsed magnetic field had been applied to the plasma arc surfacing welding on low carbon steel. The hardness, wear resistance and microstructure of surfacing layer with different pulsed magnetic field currents, duty cycles have been systematically analyzed. The results indicated that transverse alternative pulsed magnetic field can effectively improve the crystal shape of plasma arc surfacing layer, refine crystal grain. Proper pulsed magnetic field current, duty cycle can obtain the optimum effect on electromagnetic stirring which can increase the amount of hardening phase in overlay deposit, control the growth direction of hardening phase and improve the hardness and wear resistance of the surfacing overlay.

Key words: plasma arc; transverse magnetic field; microstructure; wear resistance

Investigation on welding stress and strain of titanium alloy. LI Jun[1], GUAN Qiao[2], SHI Yaowu[1] (1. Beijing Aeronautical Manufacturing Technology Research Institute, P. O. Box 863, Beijing 100024, China; 2. School of Material Science and Technology, Beijing University of Technology, Beijing 100022, China). p. 53 - 56, 60

Abstract: The welding stress and strain were investigated using the finite element method combined with the experiments. The research results showed that the metal in the melting pool is melted in the frame of area with compressive plastic strain and cooled down also in the frame of the area with compressive plastic strain. The tensile plastic strain is produced in the weld when it is in the state of 'mechanical melting' during the cooling process. But in the residual state, the compressive plastic strain still remains in the weld. The peak value of longitudinal tensile stress in the weld of titanium alloy is always lower than its yield strength at the appropriate temperature during the cooling process; this situation is kept until the residual state.

Key words: titanium alloy; welding stress; strain

Finite element anylsis of welding sequence impact on blisk roundness. ZHANG Xueqiu[1,3], YANG Jianguo[1,2], LIU Xuesong, CHEN Xuhui, FANG Hongyuan, QU Shen[2] (1. State Key Laboratory of Advanced Welding Production Technology, Harbin Institute of Technology, Harbin 150001, China; 2. Shenyang Liming Aero-Engine Group Corporation, Shenyang 110043, China; 3. Baosteel Group Corporation, Shanghai 201900, China). p. 57 - 60

Abstract: The finite element model of blisk is made by the several softwares and based on the different temperature effects during the welding process, three kinds of typical welding

sequences including welding in turn, 90° and 180° welding sequence is chosen to analyse the welding distortion. The calculation results show that 180° welding sequence is not the optimal, the welding in turn is better than the other two welding sequences under the same welding conditions. Reasonable welding sequence will change with different material welding processes and structure, which provides the theoretical basis for blisk and large-scale complex component welding sequence.

Key words: welding sequence; distortion; temperature field; residual stress

Pure titanium surface nitriding by nitrogen plasma flame

XU Wenxiao[1], TIAN Li[2], REN Zhen'an[3] (1. Key Laboratory of Advanced Structural Materials, Ministry of Education, Changchun University of Technology, Changchun 130012, China; 2. Changchun Special Equipment Inspection Center, Changchun 130000, China; 3. College of Materials Science and Engineering, Jilin University, Changchun 130025, China). p. 61—64

Abstract: A nitrogen plasma flame produced by a modified TIG welding torch was applied to heat the pure titanium specimens in the atmosphere directly and make them nitrided with the N_2+Ar plasma gas mixture, so that the nitrided layer was obtained through the interaction between Ti element of the substrate surface and N element of the plasma flame. The changes of the microstructures and properties of the nitrided layers were mainly studied by changing the nitriding temperature and nitriding time. And the better nitriding processing parameters were obtained. The mechanism of the nitrided layers and their morphologies both surface and cross-section were investigated by optical microscopy, scanning electronic microscopy, X-ray diffraction and so forth. The surface micro-hardness and the wear resistance of the nitrided layers were tested as well. The experiment and analysis results showed that the nitrided layers were mainly composed of TiN phase. The homogeneous and dense nitrided layers were well metallurgically combined with the substrate. And also they can effectively improve the wear resistance of the pure titanium substrate.

Key words: pure titanium; nitrogen plasma flame; nitrided layer

Effect of postweld heat treatment on damage mechanism of gas tungsten arc welded 308L stainless steel during creep-fatigue

LIU Feng, QI Zhenguo, HE Jun (1. School of Mechanical Engineering, Liaoning University of Petroleum & Chemical Technology, Fushun 113001, Liaoning, China; 2. Fushun City Special Equipment Supervision Inspection Agency, Fushun 113006, Liaoning, China). p. 65—68

Abstract: Strain controlled creep-fatigue tests were conducted on gas tungsten arc welded (GTAW) 308L stainless steel joints at elevated temperature. The influence of postweld heat treatment (PWHT) on the ferrite morphology and creep-fatigue behaviors of the weldment were investigated. The microstructure evolution and crack propagation behavior of the as-welded and postweld heat treated (PWHT) weldments during creep-fatigue test were examined with optical microscope (OM) and scanning electron microscope (SEM). Energy dispersive spectroscopy (EDS) was also used for intermetallic phase identification. It was found that high temperature PWHT reduced the amount of δ-ferrite in the weldment, and the creep-fatigue life increased with the increasing PWHT temperature. After high temperature PWHT, the crack propagation character was transformed from intergranular mode to mixed mode. High temperature PWHT resulted in the broken of the continuous δ-ferrite network and promoted the creep-fatigue resistance of the weldment.

Key words: stainless steel; heat treatment; creep-fatigue; damage mechanism

Synchronized record and analysis of high speed images and process parameters for welding process

CHEN Zhixiang, ZHANG Jun, SONG Yonglun, DING Yongzhong (1. College of Mechanical Engineering & Applied Electronics Technology, Beijing University of Technology, Beijing 100124, China; 2. Luoyang Ship Material Research Institute, CSIC, Luoyang 471039, Henan, China). p. 69—72, 76

Abstract: High speed camera and data acquisition are important technology to research the dynamic behavior of arc, metal transfer or weld pool in welding process. A synchronized record and analysis system for high speed images and process parameters was established based on the synchronized control for high speed camera shooting and data acquisition. The system included high speed camera, synchronous signal generator, high speed data acquisition device and synchronized player software for high speed images and waveforms. The dedicated synchronous signal generator is adequate for synchronizing and trigging high speed camera from 20 to 200 000 frames/s. The PC based data acquisition device is able to take 4 welding parameters synchronously at 200 kHz. It was demonstrated by the experiments of several typical welding processes that the system was a powerful facility for recording and analyzing the dynamic process in research on welding material, welding process, process control and stability.

Key words: high speed imaging; data acquisition; synchronized record and analysis; welding

Investigation on properties and microstructures of Ag-Cu-Zn-Sn-xGa-yIn filler metal

LAI Zhongmin[1,2], XUE Songbai[1], ZHANG Liang[1], GAO Lili[1], GU Liyong[1], GU Wenhua[3] (1. College of Materials Science and Technology, Nanjing University of Aeronautics and Astronautics, Nanjing 210016, China; 2. Province Key Lab of Advanced Welding Technology, Jiangsu University of Science and Technology, Zhenjiang 212003, Jiangsu, China; 3. Changshu Huayin Filler Metals Co., Ltd., Changshu 215513, Jiangsu, China). p. 73—76

Abstract: The effect of Ga and/or In on the microstructures of Ag based filler metals for brazing as well as the properties of the brazed joints have been investigated in this paper. Brazed with brass as the base metal (butt joints), the results showed that the optimum content of Ga and In in Ag-Cu-Zn-Sn-xGa-yIn filler metal was about 3% and 1.5% respectively, and the mechanical property of the Ag-Cu-Zn-Sn-3Ga-2In filler metal displayed the best value when the Ga and In were added into the filler metal simultaneously. When observing the tensile fracture of the butt joint brazed with Ag-Cu-Zn-Sn-3Ga-2In, it was found